Nonlocal transport mediated by nonlocal Hikami boxes: Condensation of evanescent quasiparticles injected into the superconducting gap

S. Duhot and R. Mélin
Institut NEEL, CNRS and Université Joseph Fourier, BP 166, F-38042 Grenoble Cedex 9, France
(Received 19 March 2007; published 29 May 2007)

Evanescent quasiparticles entering a superconductor and propagating over distances larger than the coherence length give rise to intermediate states induced by double Andreev scattering on disorder. The resulting effective attractive interaction between evanescent quasiparticles is retarded at the extremely slow frequency of the applied bias voltage. The out-of-equilibrium mesoscopic superconductor with a fluctuating phase variable is compatible with a recent experiment [S. Russo *et al.*, Phys. Rev. Lett. **95**, 027002 (2005)]. Microscopic theory is discussed in the random-phase approximation.

DOI: 10.1103/PhysRevB.75.184531 PACS number(s): 74.45.+c, 74.78.Na, 74.78.Fk

I. INTRODUCTION

The developments in nanotechnology allow envisioning the realization of a source of entangled pairs of electrons,[1,2] the electronic counterpart of a source of Einstein-Podolsky-Rosen pairs of photons, with possible applications to quantum information and to a test of nonlocality of quantum mechanics with electrons. Recent experiments on three-terminal devices by Beckmann *et al.*,[3] Russo *et al.*,[4] and more recently by Cadden-Zimansky and Chandrasekhar[5] realize an important step in this direction by probing crossed Andreev reflection,[6–20] in which Cooper pairs from a superconductor give rise to pairs of correlated electrons in two different ferromagnetic or normal electrodes.

Andreev reflection,[21] the mechanism by which an electron from a normal electrode is reflected as a hole at a normal-metal–superconductor interface while a pair is transmitted into the superconductor, takes place in a region of size ξ, the coherence length of the disordered superconductor. Crossed Andreev reflection (CAR) in a three-terminal normal-metal–insulator–superconductor–insulator-normal-metal (N_aISIN_b) trilayer corresponds to an Andreev process such that an electron from N_b is transmitted as a hole in N_a over a distance of order ξ, leaving a pair in the superconductor. Elastic cotunneling (EC), the other competing channel, amounts to transporting an electron from N_b to N_a without changing its spin. The two possibilities are shown schematically in Figs. 1 and 2. The nature of the dominant crossed transport channel can be controlled by the relative spin orientation of strongly polarized ferromagnets in a ferromagnet-insulator-superconductor-insulator-ferromagnet (F_aISIF_b) structure:[7,8] EC (CAR) dominates with parallel (antiparallel) spin orientations, as it can be seen from the spin of the electron or hole transmitted in electrode "N_a" (see Fig. 1). On the other hand, EC dominates for normal metals with highly transparent interfaces.[14] Crossed transport dominated either by EC or by CAR is obtained in the three recent experiments mentioned above.[3–5]

More precisely, the crossed conductance[22,23] $\mathcal{G}_{a,b}(V_b)$ of a three-terminal device measures the sensitivity of the current $I_a(V_a,V_b)$ flowing through electrode N_a with voltage V_a to the voltage V_b applied on electrode "N_b:"

$$\mathcal{G}_{a,b}(V_a,V_b)=\frac{\partial I_a(V_a,V_b)}{\partial V_b} \quad (1)$$

[see the circuit in Fig. 1]. The voltage V_a may be arbitrary, but, according to available experiments,[3–5] we consider that electrode N_a is grounded ($V_a=0$), as the superconductor.

Theoretically, the crossed conductance defined by Eq. (1) vanishes to lowest order in the tunnel amplitudes for a N_aISIN_b trilayer because the electron and hole transmitted by EC and CAR have opposite charges and because of a symmetry of crossed transport: CAR and EC have identical transmission coefficients[8,13,14] (see Fig. 2). This property does not hold for a single-channel ballistic superconductor connected by single atom contacts to normal electrodes: in this case, the crossed conductance to lowest order in the tunnel amplitudes oscillates around zero with periodicity λ_F (the Fermi wavelength) as the distance L between the contacts is varied. Oscillations in the Fermi phase factors average to zero in the realistic case of a multichannel contact[8] or in the case of a diffusive superconductor[13] with nonmagnetic impurities.

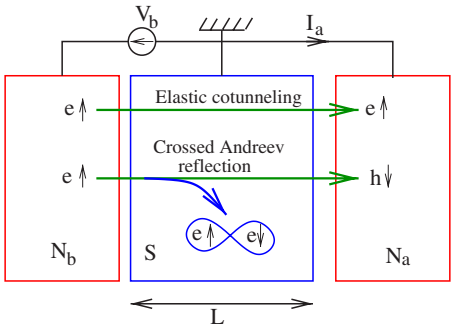

FIG. 1. (Color online) Schematic representation of the electrical circuit in a crossed transport experiment and of the two possibilities for crossed transport in a N_aISIN_b trilayer: transmission in the electron-electron channel [elastic cotunneling (EC)] and in the electron-hole channel, leaving a pair in the superconductor [crossed Andreev reflection (CAR)]. "e ↑" corresponds to a spin-up electron and "h ↓" to a hole in the spin-down band. The CAR and EC transmission coefficients decay exponentially over the coherence length as the thickness of the superconductor is increased.

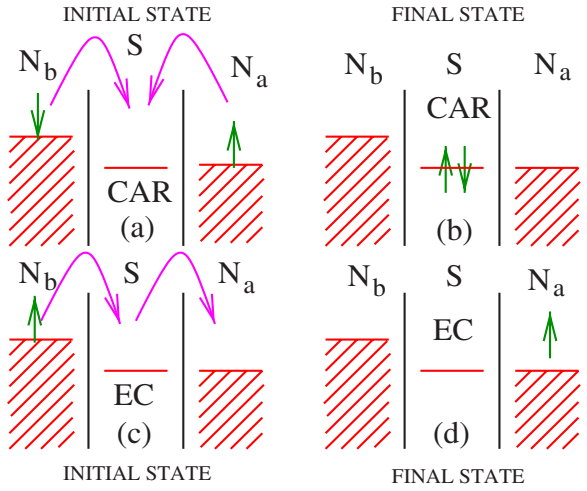

FIG. 2. (Color online) Schematic representation of the lowest-order processes: [(a) and (b)] crossed Andreev reflection (CAR) and [(c) and (d)] elastic cotunneling (EC). Not only the current through electrode N_a has an opposite sign for [(a) and (b)] CAR and [(c) and (d)] EC (as seen from the arrows on the figure), but also the CAR current is exactly opposite to the EC current for the lowest-order processes in the tunnel amplitudes (as seen from Ref. 8).

The theoretical prediction of the vanishing of the crossed conductance in a N_aISIN_b trilayer is, however, contradicted by the recent experiment by Russo *et al.*,[4] which provides an additional evidence of a disappearance of the crossed signal in a magnetic field applied parallel to the layers. A characteristic energy scale $\hbar\omega_c$ within the superconducting gap Δ is found experimentally,[4] at which the crossed signal changes sign from EC to CAR as the bias voltage energy increases above $\hbar\omega_c$ and eventually vanishes at higher energies. The experimental $\hbar\omega_c$ decreases to zero as the superconductor thickness increases. One may conjecture that such experiments are characteristic of a geometry-dependent coupling of the superconducting phase variable to crossed transport by evanescent waves. As we show, a natural possibility for such coupling (quantum interference effects in the superconductor) results in an energy scale $\hbar\omega_c$ smaller than the superconducting gap for extended junctions. Another possibility (Coulomb interactions) was put forward by Levy Yeyati *et al.* in Ref. 16 in connection with the modes of the electromagnetic environment.

II. QUANTUM INTERFERENCE EFFECT IN SUPERCONDUCTORS

A. Transmission modes related to evanescent waves

Weak localization enhances the return probability and the phase fluctuations of a normal metal.[24] A superconducting condensate is, on the contrary, delocalized and has a well defined phase. Superconductivity and weak localization are related to each other because the Cooper pairs of a superconductor can participate to the Cooperons of weak localization. Smith and Ambegaokar show indeed that the phase stiffness of a superconductor is reduced by weak localization.[25] Weak localization is, however, strongly modified in subgap transport through a superconductor by the following property of evanescent wave functions.

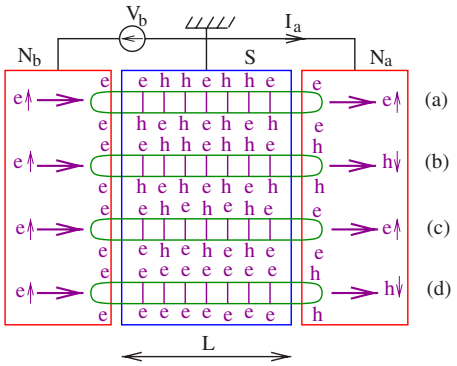

FIG. 3. (Color online) Schematic representation of the ladder series capturing the influence of disorder on the processes in Fig. 1. Examples of Nambu labels ("e" for electron and "h" for hole) are indicated on the figure [(a) and (c)] for elastic cotunneling with transmission of an electron and [(b) and (d)] for crossed Andreev reflection with transmission of a hole. e ↑ corresponds to a spin-up electron and h ↓ to a hole in the spin-down band. For clarity, the ↑ and ↓ symbols of electrons and hole are not shown for the diffusion.

Electron tunneling through a normal metal involves the simultaneous forward propagation in time of an electron and the backward propagation in time of a hole, forming a diffusion. The terminology "transmission mode" is used here for describing the effect of disorder on subgap tunneling. For evanescent states, a hole propagating backward in time can be replaced in a transmission mode by an electron propagating forward in time: the wave function of a normal electron in a box of size ξ being real valued is equal to the time reversed particle wave function in the absence of a magnetic field. Transmission modes of range ξ in subgap transport through a superconductor can thus be made also either of a pair of electrons or of a pair of holes propagating forward in time.[26] In a superconductor, a pair of electrons propagating forward in time can be obtained from a Cooper pair in the condensate.

B. Electron-hole conversion in transmission modes

As discussed in the preceding section, transmission modes in a disordered superconductor correspond to two quasiparticles scattering on the same sequence of impurities. Transmission modes are described in a standard way on the basis of ladder diagrams (see, for instance, Smith and Ambegaokar[25] in the context of localization in a superconductor). As a direct consequence of Ref. 25, intermediate states with electron-hole conversion from one impurity to the next such as in Fig. 3(c) appear as the result of *disorder scattering*, as opposed to usual Andreev reflection at a normal-metal–superconductor interface[27] being induced by *spatial variations of the superconducting pair potential*. Intermediate states with electron-hole conversion in the disordered case are, of course, not due to anomalous electron-hole scattering on impurities but due to electron-hole conversion during propagation in between two impurities.

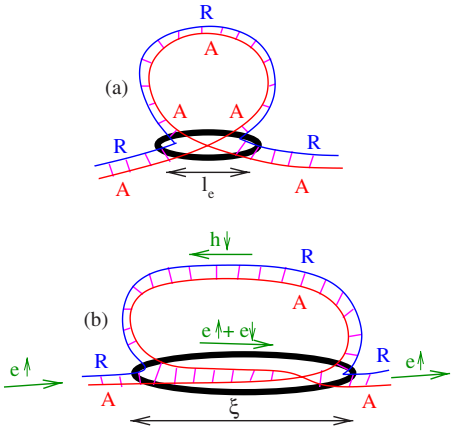

FIG. 4. (Color online) Schematic representation of transmission mode self-crossings in the presence of disorder. The circled area is the Hikami box (Refs. 28 and 29) of dimension set by the elastic mean free path l_e in a normal metal and of dimension set by the coherence length ξ for subgap transport.

For instance, transmission of an electron from electrode N_b as an electron in electrode N_a and transmission of an electron in electrode N_b as a hole in electrode N_a are shown in Figs. 3(a) and 3(b), respectively. The extreme case of a sequence of electron-hole conversions due to disorder, resulting in net transmission from electrode N_b to electrode N_a in the electron-electron channel, is shown in Fig. 3(c). Another case of net transmission of an electron in electrode N_b as a hole in electrode N_a by a sequence of normal scattering on disorder is shown in Fig. 3(d). Electron-hole conversion in between two impurities in Fig. 3(c) corresponds to a usual Andreev process, however, "interrupted" at the time scale of the elastic scattering time, leading to intermediate virtual states with a characteristic energy much above the superconducting gap. We show below that this type of intermediate-state characteristic energy scale for Andreev processes "internal" to the superconductor can be very much reduced by quantum interference effects and become observable.

C. Self-crossings of transmission modes

Self-crossings of transmission modes[28,29] are the building blocks of weak localization in the normal case[24,30] [see Fig. 4(a)]. The distinguishing features of diffusion self-crossings in subgap transport by evanescent wave functions [see Figs. 4(b) and 5(b)] were already pointed out in Ref. 17. The necessity of accounting for "advanced-advanced" or "retarded-retarded" transmission modes was already discussed by Altland and Zirnbauer[26] for an Andreev quantum dot.

Weak-localization-like loops such as in Figs. 4(b) and 5(b) contain, among all possibilities, intermediate states corresponding to double Andreev processes in which an evanescent electronlike quasiparticle (an AR transmission mode made of an advanced and a retarded Green's function for an electron propagating forward in time and a hole propagating backward in time) transforms by a first Andreev process at $\mathbf{x}_1$ in an evanescent holelike quasiparticle (another AR transmission mode for a hole propagating forward in time and an electron propagating backward in time) and the transmission

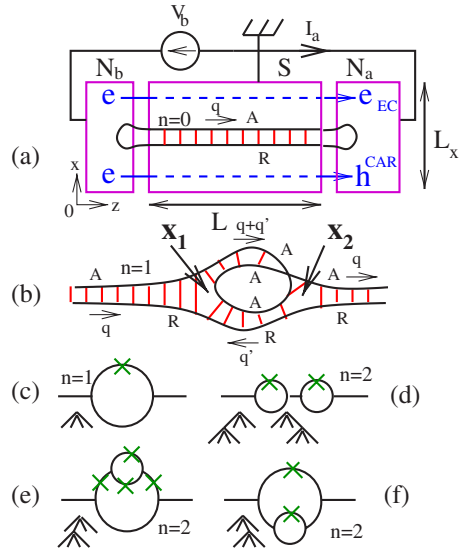

FIG. 5. (Color online) Representation of (a) the electrical circuit for crossed transport through a N_aSN_b trilayer, the electron e (top) and hole h (bottom) transmitted in electrode N_b by EC and CAR, and the "bare" transmission mode of wave vector $\mathbf{q}$ in the ladder approximation. The junction has a dimension L_y along the y axis perpendicular to the figure. The aspect ratio is not to the scale of the experiment (Ref. 4), where $L \simeq 15-200$ nm and L_x, $L_y \simeq 4$ and 8 μm. (b) A single weak-localization-like loop in a transmission mode self-crossing. The normal case is recovered for an AA transmission modes propagating locally over the elastic mean free path. (c) A compact representation of (b) and of the associated tree. The four leaves correspond to the four transmission modes making a weak-localization-like loop. AR (AA) transmission modes are represented by solid lines (with a cross). (d), (e), and (f) represent the random-phase-approximation (RPA) diagrams with $n=2$ loops and the associated trees.

of a pair (an AA transmission mode made of two advanced Green's function for a pair of electrons propagating forward in time) that recombines at $\mathbf{x}_2$ by another Andreev process after a propagation over $|\mathbf{x}_2-\mathbf{x}_1| \sim \xi$.[17] The intervention of the condensate in such loop processes is obvious from noting that the contribution of weak-localization-like processes to the crossed conductance couples to a phase gradient in the superconductor.[31] These processes result in an attractive interaction of strength v per carrier injected in the gap, in units of the Fermi energy ϵ_F. This interaction due to quantum interference effects has all the features of a *very slow* phonon exchange: it is attractive and retarded by a time $2\hbar\pi/eV_b$ (because weak-localization-like processes induces transitions only at energy $\hbar\omega=eV_b$).

As discussed previously, a transmission mode in the ladder approximation induces electron-hole conversion due to scattering on disorder, having the elastic scattering time as a characteristic time and/or inverse energy scale. Weak-localization-like loops such as in Fig. 4(b) correspond to the transport of pairs over a distance comparable to the coherence length ξ and thus have the superconducting gap Δ as a characteristic energy.[15] Similar double Andreev processes were discussed in Ref. 17 in a NISIN three-terminal device and, interestingly, were introduced previously by Jacobs and

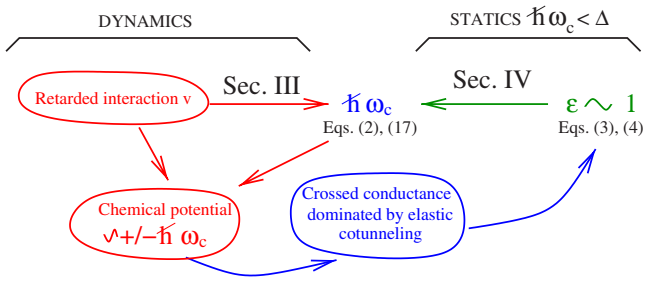

FIG. 6. (Color online) Schematic representation the link between Secs. III and IV. A characteristic energy scale $\hbar\omega_c$ is obtained from symmetry breaking between elastic cotunneling and crossed Andreev reflection ($\epsilon \sim 1$) in Eqs. (3) and (4). The energy scale $\hbar\omega_c$ is identified to the characteristic frequency for phase fluctuations in the presence of a very slow attractive interaction, which, in turn, favors a symmetry breaking in favor of elastic cotunneling.

Kümmel[32] for the time evolution of wave packets. As we show now, even smaller energy scales are obtained from many interacting weak-localization-like loops. The link between an effective dynamical model for a very slow attractive interaction in addition to the BCS pairing (Sec. III) and the resummation of many weak-localization-like loops in the static case (Sec. IV) is shown schematically in Fig. 6.

III. SLOW ATTRACTIVE INTERACTION IN A SUPERCONDUCTOR

A. Energy scale within the gap

Changing the phase by $\pm 2\pi$ during a time interval $2\pi/\omega_c$ requires the time $2\pi/\omega_c$ to be smaller than $2\pi\hbar/eV_b$, the retardation in the interactions that prevent the phase from fluctuating. The BCS case with a phase constant in time corresponds to retarded interactions with a Debye energy $\hbar\omega_D$, orders of magnitude larger than the superconducting gap Δ. In the opposite limit $eV_b < \hbar\omega_c$ that we consider, the interaction v has to visit and fix the phase of a number of states $N(0)\hbar\omega_c$ in the normal metal to rotate the phase by 2π within a delay $2\pi/\omega_c$, with $N(0)=2\pi LL_xL_y/\lambda_F^3\epsilon_F$ the number of normal states per unit energy and with ϵ_F the Fermi energy and λ_F the Fermi wavelength (see L, L_x, and L_y in Fig. 5). By the uncertainty relation $v\epsilon_F\Delta t=\hbar$, the effective number of interactions in a time interval $2\pi/\omega_c$ is $N_{int}(\omega_c)=2\pi/\omega_c\Delta t=2\pi v\epsilon_F/\hbar\omega_c$. The characteristic energy $\hbar\omega_c$ is obtained by equating $N_{int}(\omega_c)=N(0)\omega_c$:

$$\frac{\hbar\omega_c}{\epsilon_F} = \sqrt{\frac{v\lambda_F^3}{LL_xL_y}}. \tag{2}$$

The decoupling between $\hbar\omega_c$ and the states at energy larger than Δ is justified if $\hbar\omega_c \ll \Delta$, which we suppose in the following. The superconducting phase fluctuates by $\pm 2\pi$ with a frequency ω_c, but its average value over a time window larger than the retardation of interactions $2\pi\hbar/eV_b$ does not fluctuate. The Andreev current from the superconductor to electrode N_a vanishes for $eV_b < \hbar\omega_c$ because the superconductor chemical potential fluctuates between typical values $\pm\hbar\omega_c$. The crossed conductance is then dominated by EC, as it can be seen from second-order perturbation theory in the tunnel amplitudes[33] (see Fig. 7).

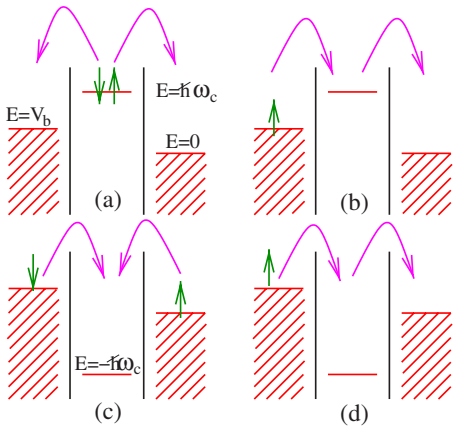

FIG. 7. (Color online) Schematic representation the lowest-order processes for superconductor chemical potentials $\hbar\omega_c$ [(a) and (b)] larger than eV_b or [(c) and (d)] smaller than eV_b. The crossed Andreev reflection (CAR) processes (a) and (c) lead to opposite crossed currents for superconductor chemical potentials $\simeq\pm\hbar\omega_c$, while the elastic cotunneling (EC) processes (b) and (d) result in additive crossed currents. The crossed conductance with a superconductor chemical potential fluctuating between $\simeq\pm\hbar\omega_c$ is thus dominated by EC.

B. Qualitative behavior of the crossed conductance

We consider now the case $eV_b \gtrsim \hbar\omega_c$. The proximity of the characteristic energy $\hbar\omega_c$ induces pair correlations among evanescent quasiparticles injected in the superconductor at bias voltage energies $eV_b \gtrsim \hbar\omega_c$. CAR and EC processes are described schematically:[33] (b), (c), and (d) in the inset of Fig. 8 correspond to acting twice with the tunnel Hamiltonian, starting from the superconductor in the BCS ground state for (b) and with a correlated pair in the initial state for (c) and (d). The crossed signals due to the EC and CAR processes (c) and (d) cancel each other out because (c) involves an extra anticommutation of fermions compared to (d). The EC process (c) cancels with a CAR process (not shown in Fig. 8) in which two electrons at energies $-eV_b$ and eV_b in electrodes N_a and N_b enter the superconductor as a pair. Fluctuations by one quasiparticle with spin σ in the superconductor do not couple to the crossed signal because EC has an opposite sign for the two orientations of σ. The remaining contribution to the crossed signal (not shown in Fig. 8) is due to tunneling of the two electrons of a correlated pair from the superconductor to electrode N_a, leading to a negative differential crossed resistance, as for local Andreev reflection above the superconducting gap in a NIS junction.[27] From these arguments, we conclude that a change of sign from a positive EC crossed resistance for $eV_b < \hbar\omega_c$ to a negative Andreev reflection crossed resistance for $eV_b \gtrsim \hbar\omega_c$ occurs and that the crossed signal disappears at higher energies, as in experiments.[4]

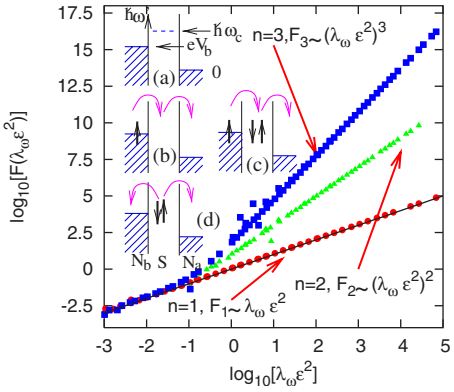

FIG. 8. (Color online) Scaling plot of $F_n(\lambda_\omega \epsilon^2)$ as a function of $\lambda_\omega \epsilon^2$ for diagrams with $n=1$ (•), $n=2$ (▲), and $n=3$ (■) weak-localization-like loops. The energy $\hbar\omega$ and the dimensionless symmetry breaking parameter ϵ vary over 3 orders of magnitude. The values of the elastic mean free path l_e, such that $2 \leqslant \xi/l_e \leqslant 14$ (as compared to $\xi/l_e=5-7$ in the experiment[4]), vary from the dirty limit to the crossover with the ballistic limit. For clarity, not all calculated points are shown on the figure. (a) shows one value $2\pi/\omega_c$ of the superconductor chemical potential. (b), (c), and (d) show EC and CAR processes for $eV_b \gtrsim \hbar\omega_c$ with residual pair correlations among evanescent quasiparticles.

IV. RANDOM-PHASE APPROXIMATION FOR WEAK-LOCALIZATION-LIKE PROCESSES

A. Method and algorithm

1. Crossed conductance and resistance

Now, we start from a static superconducting gap (see Fig. 6) and determine from microscopic theory the analog of Eq. (2) for a dirty superconductor. We denote by $T_{CAR}(\mathbf{R},\omega)$ and $T_{EC}(\mathbf{R},\omega)$ the CAR and EC dimensionless transmission coefficients of a superconductor at distance $\mathbf{R}$ and energy $\hbar\omega$ below the gap corresponding, respectively, to electron and hole transmissions (see Figs. 1 and 2) described by transmission modes in the ladder approximation such as in Fig. 3.

We enforce a finite crossed current by breaking the symmetry $T_{EC}(\mathbf{R},\omega)=T_{CAR}(\mathbf{R},\omega)$ according to

$$T_{EC}(\mathbf{R},\omega) = T_0(\mathbf{R},\omega)(1+\epsilon), \tag{3}$$

$$T_{CAR}(\mathbf{R},\omega) = T_0(\mathbf{R},\omega)(1-\epsilon). \tag{4}$$

The crossed conductance per conduction channel,

$$\mathcal{G}_{a,b}(\mathbf{R},\omega) = -2\left(\frac{e^2}{h}\right)\mathcal{T}^2 T_{ch}(\mathbf{R},\omega), \tag{5}$$

corresponds to processes of lowest order $\mathcal{T}^2$ in an expansion in the dimensionless interface transmission coefficient $0<\mathcal{T}<1$, and the charge transmission coefficient of the superconductor, $T_{ch}(\mathbf{R},\omega)=T_{EC}(\mathbf{R},\omega)-T_{CAR}(\mathbf{R},\omega)$, accounts for the different carriers transmitted by EC and CAR in electrode N_a. The resulting crossed resistance per channel is obtained as the inverse of the extra diagonal element of the inverse of the crossed conductance matrix:

$$\begin{bmatrix} \mathcal{R}_{a,a} & \mathcal{R}_{a,b} \\ \mathcal{R}_{b,a} & \mathcal{R}_{b,b} \end{bmatrix} = \begin{bmatrix} \mathcal{G}_{a,a} & \mathcal{G}_{a,b} \\ \mathcal{G}_{b,a} & \mathcal{G}_{b,b} \end{bmatrix}^{-1}, \tag{6}$$

with

$$\mathcal{G}_{a_i,a_j}(V_a,V_b) = \frac{\partial I_{a_i}}{\partial V_{a_j}}(V_a,V_b) \tag{7}$$

generalizing Eq. (1), where the entries a_i and a_j in Eq. (7) correspond to the labels a and b of the normal electrodes N_a and N_b. We deduce from Eq. (6) the off-diagonal matrix element of the crossed resistance matrix:

$$\mathcal{R}_{a,b} = -\frac{\mathcal{G}_{a,b}}{\mathcal{G}_{a,a}\mathcal{G}_{b,b}-\mathcal{G}_{a,b}\mathcal{G}_{b,a}}, \tag{8}$$

approximated as

$$\mathcal{R}_{a,b} \simeq -\frac{\mathcal{G}_{a,b}}{\mathcal{G}_{a,a}\mathcal{G}_{b,b}}, \tag{9}$$

because of the damping of crossed processes over the coherence length ξ. The dependence on V_a and V_b is not explicit in Eqs. (8) and (9). We obtain the following from Eq. (5):

$$\mathcal{R}_{a,b}(\mathbf{R},\omega) \simeq \left(\frac{h}{2e^2}\right)\mathcal{T}^{-2} T_{ch}(\mathbf{R},\omega), \tag{10}$$

much larger than for our previous approach for higher-order processes at the interfaces.[15,17]

2. Algorithm

The excitations of the condensate, integrated out by the random-phase approximation[34] (RPA) for the transmission modes, lead to a new value of the crossed conductance corresponding to replacing ϵ by $\tilde{\epsilon}(\mathbf{R},\omega,\epsilon)$. We identify the characteristic energy $\hbar\omega_c$ as the divergence in the energy dependence of $\tilde{\epsilon}(\mathbf{R},\omega,\epsilon)$, as for a gap edge singularity. The symmetry breaking parameter $\tilde{\epsilon}_n(\mathbf{R},\omega,\epsilon)$ with n localization loops is obtained by inverting

$$\tilde{T}_{EC}(n,\epsilon) = \tilde{T}_0(n) + \tilde{\epsilon}_n(\epsilon)T_0, \tag{11}$$

$$\tilde{T}_{CAR}(n,\epsilon) = \tilde{T}_0(n) - \tilde{\epsilon}_n(\epsilon)T_0, \tag{12}$$

with n the number of weak-localization-like loops, and where the dependence on $\mathbf{R}$ and ω is not explicit in Eqs. (11) and (12). We deduce the value of

$$F_n(\mathbf{q},\omega,\epsilon) \equiv \frac{\tilde{\epsilon}_n(\mathbf{q},\omega,\epsilon)}{\epsilon} - 1, \tag{13}$$

where we changed variable from $\mathbf{R}$ to the wave vector $\mathbf{q}$ by a Fourier transform.

An algorithm generates the topologically inequivalent higher-order RPA diagrams for the transmission mode with the tree structure shown in Figs. 5(c)–5(f). These diagrams maximizing the number of imbricated loops for a given number of branchings are the most relevant for describing intermediate states with a proliferation of Andreev reflections internal to the superconductor for $\omega \simeq \omega_c$. In order to reduce

the computation time, we first specialize to a single channel by restricting to the transverse components $(q_x', q_y', q_z') = (0, 0, 2\pi n_z/L)$ of the wave vector $\mathbf{q}' = (q_x', q_y', q_z') = (2\pi n_x/L_x, 2\pi n_y/L_y, 2\pi n_z/L)$ in the weak-localization-like loop, with n_x, n_y, and n_z are three integers (see Fig. 5). The scaling with the number of longitudinal components is restored afterward.

B. Results

Now, we present the result of RPA resummation. The $\mathbf{q}$ dependence of the transmission coefficients is, up to an overall rescaling, the same as for the bare transmission coefficient, because of the properties of the convolution of exponentials in the corresponding transmission coefficients in real space. We thus evaluate only the rescaling factor $F_n(0, \omega, \epsilon)$ that collapses on master curves (see Fig. 8) when plotted as a function of the dimensionless parameter

$$\lambda_\omega \epsilon^2 = k_F L \left(\frac{\hbar \omega \epsilon}{\epsilon_F} \right)^2 (k_F l_e)^{2\alpha}, \tag{14}$$

according to $F_n(0, \omega, \epsilon) \equiv F_n(\lambda_\omega \epsilon^2)$, with l_e the elastic mean free path such that $2 \leqslant \xi/l_e \leqslant 14$ and with $\alpha = 1.1 \pm 0.1$. Summing the RPA diagrams leads to $\tilde{\epsilon}$, the new value of ϵ modified by the response of the condensate:

$$\tilde{\epsilon}(\omega, \epsilon) = \epsilon [1 + F_\infty(\lambda_\omega \epsilon^2)] = \frac{\epsilon}{1 - \lambda_\omega \epsilon^2}. \tag{15}$$

V. IDENTIFICATION OF THE ENERGY SCALES

A. Characteristic energy of a disordered superconductor

To take into account the large longitudinal dimensions of the junction, we note that convolutions of the exponential envelope of the transmission coefficients lead to an enhancement of $\lambda_\omega \epsilon^2$ by a factor $k_F^2 L_x L_y$ for extended interfaces. More precisely, combining diffusion modes for 0 to x and from x to L leads to convolutions of the form

$$\int_0^L \exp(-x/\xi) \exp(-(L-x)/\xi) dx = L \exp(-L/\xi), \tag{16}$$

where the one-dimensional case with two evanescent diffusion modes is considered for simplicity.

We deduce from Eq. (14) the characteristic energy $\hbar\omega_c$ of a dirty superconductor:

$$\frac{\hbar \omega_c}{\epsilon_F} = \frac{1}{|\epsilon|} \frac{1}{(k_F l_e)^\alpha} \frac{1}{\sqrt{k_F^3 L L_x L_y}}. \tag{17}$$

The parameter of interactions v in Eq. (2) is independent of Δ, as expected for a mechanism due to electron-hole conversion below the gap;[27] the lowest of the characteristic energy $\hbar\omega_c$ and the voltage eV_b, rather than $v\epsilon_F$, is an indicator of the strength of weak-localization-like quantum interference effect in subgap transport. The form of the transmission coefficients puts the constraint $|\epsilon| < 1$. The value $\epsilon = 1$ favoring EC with respect to CAR and minimizing $\hbar\omega_c$ in Eq. (17) for a static superconducting gap is compatible with the previous picture of a fluctuating chemical potential (see Fig. 6) and with the large EC crossed signal measured experimentally at zero bias in Ref. 4.

B. Comparison with experiments

We use $l_e \simeq 2$ nm from Ref. 4, $\epsilon_F \simeq 5.3$ eV, and $k_F \simeq 1$ Å^{-1} for Nb. In experiments, $\hbar\omega_c$ is limited by $l_\varphi \simeq 0.1$–0.2 μm [as obtained from the inelastic electron-electron scattering time $\tau_{e-e} \simeq 1$ ns (Ref. 4)], instead of the sample dimensions L_x and L_y in Eq. (17), leading to $\hbar\omega_c \simeq 21$–10, 11–6, and 6–3 μeV for $L \simeq 15$, 50, and 200 nm, respectively. Russo *et al.*[4] found experimentally $\hbar\omega_c \simeq 270$ and 50 μeV for $L \simeq 15$ and 50 nm and $\hbar\omega_c$ below the resolution threshold for $L \simeq 200$ nm. The theoretical approximation underestimates the experimental $\hbar\omega_c$ in the regime $L \sim \xi$ ($L = 15$ and 50 nm and $\xi = 10$–15 nm in experiments[4]). The energy scale Δ is associated with objects of size $\lesssim \xi$ formed by the accommodated weak-localization-like loops for $L \simeq \xi$. The energy scale $\hbar\omega_c$ is thus enhanced by a crossover to perturbative effects of weak-localization-like loops, with $\hbar\omega_c$ reaching $\sim\Delta$ for $L \sim \xi$, as in the absence of weak-localization-like loops.[14,17] The crossover is not captured by Eq. (17) with $L \gg \xi$.

VI. CONCLUSIONS

In summary, intermediate states due to double Andreev processes induced by a weak-localization-like quantum interference effect in subgap transport are at the root of a very slow attractive interaction between evanescent quasiparticles. The interaction arises in an out-of-equilibrium situation if quasiparticles are forced to travel through the superconductor over distances exceeding the coherence length ξ, which does not apply to usual Andreev reflection limited by ξ. The phase of the mesoscopic superconductor fluctuates with a characteristic time $2\pi/\omega_c$ if the bias voltage energy eV_b is smaller than $\hbar\omega_c$, because of the large retardation $\hbar/eV_b$ in double Andreev processes due to weak-localization-like loops, as opposed to interactions retarded over the Debye frequency for a BCS superconductor. The model explains the following experimental facts: (i) the existence of an energy scale $\hbar\omega_c$ within the superconducting gap, decaying to zero as the superconductor thickness L increases; (ii) a change of sign from EC for $eV_b < \hbar\omega_c$ to CAR for $eV_b > \hbar\omega_c$ and a disappearance of the crossed signal for $\hbar\omega_c$ larger than a few $\hbar\omega_c$; and (iii) the coupling of weak-localization-like quantum interference effect to a magnetic field. A challenging issue is to account for the interplay between weak-localization-like quantum interference effect discussed here and the coupling to the electromagnetic field.[16]

ACKNOWLEDGMENTS

The authors acknowledge crucial discussion with B. Douçot, D. Feinberg, M. Houzet, F. Pistolesi, and J. Ranninger and thank H. Courtois, S. Florens, and K. Matho for useful remarks on the paper.

[1] M. S. Choi, C. Bruder, and D. Loss, Phys. Rev. B **62**, 13569 (2000); P. Recher, E. V. Sukhorukov, and D. Loss, *ibid.* **63**, 165314 (2001).
[2] G. B. Lesovik, T. Martin, and G. Blatter, Eur. Phys. J. B **24**, 287 (2001); N. M. Chtchelkatchev, G. Blatter, G. B. Lesovik, and T. Martin, Phys. Rev. B **66**, 161320(R) (2002).
[3] D. Beckmann, H. B. Weber, and H. v. Löhneysen, Phys. Rev. Lett. **93**, 197003 (2004).
[4] S. Russo, M. Kroug, T. M. Klapwijk, and A. F. Morpurgo, Phys. Rev. Lett. **95**, 027002 (2005).
[5] P. Cadden-Zimansky and V. Chandrasekhar, Phys. Rev. Lett. **97**, 237003 (2006).
[6] J. M. Byers and M. E. Flatté, Phys. Rev. Lett. **74**, 306 (1995).
[7] G. Deutscher and D. Feinberg, Appl. Phys. Lett. **76**, 487 (2000).
[8] G. Falci, D. Feinberg, and F. Hekking, Europhys. Lett. **54**, 255 (2001).
[9] P. Samuelsson, E. V. Sukhorukov, and M. Büttiker, Phys. Rev. Lett. **91**, 157002 (2003).
[10] E. Prada and F. Sols, Eur. Phys. J. B **40**, 379 (2004).
[11] P. K. Polinák, C. J. Lambert, J. Koltai, and J. Cserti, Phys. Rev. B **74**, 132508 (2006).
[12] T. Yamashita, S. Takahashi, and S. Maekawa, Phys. Rev. B **68**, 174504 (2003).
[13] D. Feinberg, Eur. Phys. J. B **36**, 419 (2003).
[14] R. Mélin and D. Feinberg, Phys. Rev. B **70**, 174509 (2004).
[15] R. Mélin, Phys. Rev. B **73**, 174512 (2006).
[16] A. Levy Yeyati, F. S. Bergeret, A. Martin-Rodero, and T. M. Klapwijk, arXiv:cond-mat/0612027, Nat. Phys. (to be published).
[17] S. Duhot and R. Mélin, Eur. Phys. J. B **53**, 257 (2006).
[18] J. P. Morten, A. Brataas, and W. Belzig, Phys. Rev. B **74**, 214510 (2006).
[19] F. Giazotto, F. Taddei, F. Beltram, and R. Fazio, Phys. Rev. Lett. **97**, 087001 (2006).
[20] A. Brinkman and A. A. Golubov, Phys. Rev. B **74**, 214512 (2007).
[21] A. F. Andreev, Sov. Phys. JETP **19**, 1228 (1964).
[22] C. J. Lambert and R. Raimondi, J. Phys.: Condens. Matter **10**, 901 (1998).
[23] F. J. Jedema, B. J. van Wees, B. H. Hoving, A. T. Filip, and T. M. Klapwijk, Phys. Rev. B **60**, 16549 (1999).
[24] E. Akkermans and G. Montambaux, *Physique Mésoscopique des Électrons et des Photons*, CNRS ed. (EDP Sciences, Paris, 2004).
[25] R. A. Smith and V. Ambegaokar, Phys. Rev. B **45**, 2463 (1992).
[26] A. Altland and M. R. Zirnbauer, Phys. Rev. B **55**, 1142 (1997).
[27] G. E. Blonder, M. Tinkham, and T. M. Klapwijk, Phys. Rev. B **25**, 4515 (1982).
[28] L. P. Gorkov, A. Larkin, and D. E. Khmelnitskii, Pis'ma Zh. Eksp. Teor. Fiz. **30**, 248 (1979) [JETP Lett. **30**, 228 (1979)].
[29] S. Hikami, Phys. Rev. B **24**, 2671 (1981).
[30] A Hikami box in subgap transport contains an "AA" diffusion made of two advanced Green's functions, ending by two crossings between three diffusions (Ref. 17).
[31] S. Duhot and R. Mélin, arXiv:cond-mat/0701748 (unpublished).
[32] A. Jacobs and R. Kümmel, Phys. Rev. B **64**, 104515 (2001).
[33] B. I. Spivak and S. A. Kivelson, Phys. Rev. B **43**, 3740 (1991).
[34] P. W. Anderson, Phys. Rev. **112**, 1900 (1953).